# ANALYSIS OF BLOOD VESSEL TOPOLOGY BY CUBICAL HOMOLOGY

[†]*M. Niethammer,* [†]*A. N. Stein,* [‡]*W. D. Kalies,* [◇⋆]*P. Pilarczyk,* [◇]*K. Mischaikow,* [†]*A. Tannenbaum*

Georgia Institute of Technology
[†]School of Electrical and Computer Engineering
Atlanta, GA, 30332-0250, USA

Florida Atlantic University
[‡]Department of Mathematical Sciences
Boca Raton, FL, 33431, USA

Georgia Institute of Technology
[◇]School of Mathematics
Atlanta, GA, 30332-0160, USA

Jagiellonian University
[⋆] Institute of Computer Science
30-072 Kraków, Poland

## ABSTRACT

In this note, we segment and topologically classify brain vessel data obtained from magnetic resonance angiography (MRA). The segmentation is done adaptively and the classification by means of cubical homology, i.e. the computation of homology groups. In this way the number of connected components (measured by $H_0$), the tunnels (given by $H_1$) and the voids (given by $H_2$) are determined, resulting in a topological characterization of the blood vessels.

## 1. INTRODUCTION

Many computer application areas involve topological questions: image processing, cartography, computer graphics, molecular modeling to name but a few [1]. The main reason for the application of topological methods is their significant reduction in the amount of data. The emphasis is on shape as opposed to metric. One approach for the computation of topological information from image data is the theory of cubical homology [2]. Cubical homology lends itself naturally to image processing, since it deals directly with the voxels in three-dimensional images. No additional triangulation is necessary, facilitating efficient computer algorithms for the computation of the cubical homology.

In this note, the cubical homology approach is used to analyze three-dimensional magnetic resonance angiographs of brain blood vessels. Since simple thresholding (to separate the blood vessels from the overall brain image) of a gray-level image may not lead to satisfactory results, we use an adaptive thresholding algorithm (described in Section 2). The thresholding yields a binary segmentation, with the interior of the blood vessels represented as solids. This binary segmented image constitutes the input data for the homology computation; see Section 3. Section 4 presents the result of the combined segmentation/homology algorithm for the blood vessel image. The paper concludes with a summary (see Section 5), an outlook on future work, and work under progress.

## 2. ADAPTIVE THRESHOLDING

The segmentation of the data is performed using a knowledge-based approach [3, 4, 5]. By means of a modified Bayesian maximum *a posteriori* (MAP) algorithm (to be described below), the pixels of each cross sectional image are classified as either vessel or background. According to Bayes' Rule, the posterior probability that a given pixel belongs to a particular class $c$, given its intensity $v$ is:

$$\Pr(C_i = c|V_i = v) = \frac{\Pr(V_i = v|C_i = c)\ \Pr(C_i = c)}{\sum_\gamma \Pr(V_i = v|C_i = \gamma)\ \Pr(C_i = \gamma)}. \quad (1)$$

Note that the denominator serves simply as a normalizing factor. This normalization is automatically enforced in our implementation, and so its explicit calculation is unnecessary.

More precisely, the *a priori* class likelihood for each pixel is defined as a uniform distribution over the available classes. Posterior probabilities for each class are then calculated based on Gaussian distributions. Given initial means and standard deviations, the likelihood of a particular pixel $i$ having a certain value $v$ given that it is in class $c \in \{vessel, background\}$ is:

$$\Pr(V_i = v|C_i = c) = \frac{1}{\sqrt{2\pi}\sigma_c} \exp\left(-\frac{1}{2}\frac{(v-\mu_c)^2}{\sigma_c^2}\right). \quad (2)$$

Each class's posteriors calculated according to Bayes' Rule (1), are then anisotropically smoothed using the affine heat

equation filter

$$\frac{\partial P^c}{\partial t} = ((P_y^c)^2 P_{xx}^c - 2P_x^c P_y^c P_{xy}^c + (P_x^c)^2 P_{yy}^c)^{1/3}. \quad (3)$$

(Three iterations of the filter were sufficient. After each iteration the two probabilites were renormalized so that their sum would be one.) Then the maximum posterior probability at each pixel is chosen for the final segmentation by:

$$C_i^* = \underset{c \in \{vessel, background\}}{\arg\max} \Pr^*(C_i = c | V_i = v), \quad (4)$$

where $\Pr^*$ is the smoothed version of the posteriors. As the algorithm progresses through the set of 2D slices, posteriors from one slice are used as the priors for the next slice. In addition, a small amount of smoothing along the cross-sectional axis is used, and the Gaussian distribution parameters for each class are updated according to the results of the last segmentation. Together, these enforce continuity and provide for knowledge transfer between the slices. In this way, the system effectively "learns" the appropriate class and intensity distributions as it advances through the data set.

One important aspect of the posterior to prior transfer is the use of a lower limit. To allow for new structures to develop in the segmentation, priors are set equal to the previous posterior probabilities *or* a given minimum value, whichever is greater. This prevents regions of zero-probability from arising, which would inhibit such structures from having sufficiently large posteriors to be classified via the MAP approach.

## 3. CUBICAL HOMOLOGY

Cubical homology is ideally suited for digital images, due to its ability to handle voxels or pixels directly. Whereas homology is by now a standard tool of algebraic topology (cf. [6]), cubical homology is more recent [7, 8]. Homology aims at counting holes in a topological space. For three-dimensional image data (as investigated in this note) three non-trivial homology groups $H_0$, $H_1$ and $H_2$ exist. The number of connected components, tunnels and voids present in the image are given by the Betti numbers $\beta_0$, $\beta_1$ and $\beta_2$ respectively; where $\beta_i$ is the rank of the homology group $H_i$.

MRA was used to produce a 256 by 256 by 41 volumetric image of the brain. Thus the raw data consists of $256 \times 256 \times 41$ voxels each of which is assigned a gray scale between 0 and 255. As was noted above our goal is to classify the topological structure of the blood vessels. Consider for the moment the following idealized version of the problem. Let $X = [0, 256] \times [0, 256] \times [0, 41]$ represent the region being imaged and let $g : X \to \mathbf{R}$ be a smooth function whose values are the gray scales of the image. Furthermore, assume that there is a unique gray scale value $s_0$ which corresponds to the blood vessels. Then, the blood vessels are given by $B = g^{-1}(s_0)$. Observe that since one would expect $g$ to be a highly nonlinear function, even this idealized implicit description of $B$ does not shed light on the structure of the vessels. For this reason we turn to homology.

As was noted earlier, the ranks of homology groups $H_0(B)$, $H_1(B)$, and $H_2(B)$ provide information on the number of distinct pieces, tunnels, and bounded regions in $X$ defined by $B$. An obvious question at this point, is how sensitive are the homology groups to perturbations of $B$. We can ask this question in two ways: (1) let $f : X \to \mathbf{R}$ be a perturbation of $g$ and let $B' = f^{-1}(s_0)$, or (2) let $B' = g^{-1}(s_1)$ where $s_1 \neq s_0$. Morse theory [9] guarantees that if $f$ and $g$ are sufficiently close or if there are no critical values of $g$ in the interval $[s_0, s_1]$, then $H_*(B)$ and $H_*(B')$ are the same. In fact, in the latter case, if $B'' := g^{-1}([s_0, s_1])$, then $H_*(B)$ is the same as $H_*(B'')$.

Ignoring the noise, the raw data differs from the idealized version in two fundamental points. First, the gray scales associated to the vessels are not confined to a single value, and second, the data takes a constant value on each voxel and changes discontinuously from voxel to voxel. The last comment of the previous paragraph indicates that if the range of the gray scales representing the blood vessels is not too large, then the homology is well defined. The second issue is overcome by the fact that homology is a combinatorial theory, i.e. it can be computed by decomposing the space into a finite number of units. In the traditional simplicial homology, these units are simplices. In the cubical homology these units are pixels/voxels and their respective vertices, edges and higher-dimensional faces.

Formally, an *elementary cube* Q is given by the finite product [10]

$$Q = I_1 \times I_2 \times \cdots \times I_d \subset \mathbb{R}^d, \quad (5)$$

where $I_i$ is either a singleton (*degenerated*) interval $I = [l, l] = [l]$ or an interval of unit length $I = [l, l + 1]$ for some $l \in \mathbb{Z}$. The number of non-degenerate components in $Q$ is called the *dimension* of $Q$ ($\dim Q$). If a set $X \subset \mathbb{R}^d$ can be written as a finite number of elementary cubes, it is called a *cubical* set. The set of all elementary cubes in $\mathbb{R}^d$ is denoted by $\mathcal{K}$, and the set of all elementary cubes $Q$ with $\dim Q = k$ by $\mathcal{K}_k$, for $k \in \mathbb{N}$.

**Definition 1**
*Let $X \subset \mathbb{R}^d$ be a cubical set. Let*

$$\mathcal{K}(X) := \{Q \in \mathcal{K} \mid Q \subset X\} \text{ and}$$
$$\mathcal{K}_k(X) := \{Q \in \mathcal{K}(X) \mid \dim Q = k\}.$$

To pass from the combinatorial structure of the elementary cubes, e.g. the collection of voxels, to the algebraic structure

of homology groups, one constructs the free abelian group of $k$-chains, $C_k(X)$ by declaring each element of $\mathcal{K}_k(X)$ to be a distinct generator (or basis element). Let $C_k$ denote $C_k(\mathcal{R}^d)$.

Given $k \in \mathbb{Z}$, the cubical boundary operator

$$\partial_k : C_k \to C_{k-1} \tag{6}$$

is the group homomorphism defined on every elementary cube $Q \in \mathcal{K}_k$ as the alternating sum of its $(k-1)$-dimensional faces. Due to linearity this boundary operator extends to all k-chains. A k-chain $z \in C_k(X)$ is called a *cycle* in $X$ if $\partial_k z = 0$. A k-chain $z \in C_k(X)$ is called a *boundary* in $X$ if there exists a $c \in C_{k+1}(X)$ such that $\partial_{k+1} c = z$. The set of all cycles and the set of all boundaries in $X$ form subgroups in $C_k(X)$ and are given by

$$Z_k(X) := \ker \partial_k^X = C_k(X) \cap \ker \partial_k \tag{7}$$

$$B_k(X) := \text{image } \partial_{k+1}^X = \partial_{k+1}\left(C_{k+1}(X)\right) \tag{8}$$

respectively.

**Definition 2**
*The k-th* cubical homology group *of $X$ is the quotient group*

$$H_k(X) := Z_k(X)/B_k(X).$$

The Betti numbers $\beta_k$ are then given as

$$\beta_k := \text{rank}(H_k(X)). \tag{9}$$

The elements of $H_k(X)$ are called the *k-generators of the homology module of $X$*. The homology groups are computed as (for example) described in [8]. Generators and Betti numbers facilitate the topological characterization of the dataset (see Section 4).

## 4. COMPUTATIONAL RESULTS

The computation was performed on a 256 by 256 by 41 volumetric image of the brain obtained by angiography provided by the Surgical Planning Lab of Brigham and Women's Hospital. Figure (1) shows two exemplatory sagital slices through the brain. The complete three-dimensional image was segmented (see Section 2); see Figure (2) for a rendered image of the segmentation. The Betti numbers were then computed from the binary images, with $\beta_0 = 16$ representing the number of connected components, i.e. the number of detected vessels/vessel-parts. To compute the generators, the hull of the binary image was generated to yield tunnels representing the vessels. In a preliminary processing step the cubes of the inverted binary image were contracted, reducing the number of cubes from $15{,}625$ initially to $870$. The homology was computed from the contracted representation, and resulted in the Betti numbers $\beta_0 = 9$, $\beta_1 = 8$ and $\beta_2 = 22$, corresponding to nine connected components, eight tunnels (vessels that run from one boundary of the cuboid to another and branches of these vessels) and 22 voids (the vessel parts that are unconnected and lie entirely in the cuboid). The actual computation of the homology of the complex took about 3 seconds on a Sun Ultra 60 with 512 MB of RAM. Figure (3) shows the skeleton of the cubical complex of the vessels overlaid by the computed one-generators. They enclose the vessels, but are neither minimal nor do they necessarily enclose just one branch of a vessel. To ensure these two properties further research is needed and is currently being conducted.

## 5. CONCLUSION

In this paper we used an adaptive thresholding algorithm to segment vessels from an MRA image. The topology (Betti numbers and generators) of the binary segmented three-dimensional image was calculated and illustrated by an image of the skeleton of the complex including a set of one-generators. Future work will deal with the computation of minimal generators and their positioning along the branches of the vessels. The authors believe that the method has the potential of becoming a valuable tool for many application areas, reducing information that is difficult to grasp visually to topological key quantities. Furthermore, since the homology computations are dimension independent, the analysis of higher dimensional data (e.g. 4D-data) will become feasible, which would be even more demanding to assess visually.

## 6. REFERENCES


[1] T. K. Dey, H. Edelsbrunner, and S. Guha, "Computational topology," in *Advances in Discrete and Computational Geometry*, B. Chazelle, J. E. Goodman, and R. Pollack, Eds., Contemporary Mathematics, pp. 109–143. American Mathematical Society, 1999.

[2] M. Allili, K. Mischaikow, and A. Tannenbaum, "Cubical homology and the topological classification of "2D" and "3D" imagery," in *Proceedings of the International Conference on Image Processing*. IEEE, 2001, vol. 2, pp. 173–176.

[3] S. Haker, G. Sapiro, and A. Tannenbaum, "Knowledge-based segmentation of SAR data with learned priors," *IEEE Transactions on Image Processing*, vol. 9, pp. 298–302, 2000.

[4] S. Haker, G. Sapiro, A. Tannenbaum, and D. Wasburn, "Missile tracking using knowledge-based adaptive thresholding," in *Proceedings of the International Conference on Image Processing*. IEEE, 2001, pp. 786–789.

[5] P. Teo, G. Sapiro, and B. Wandell, "Creating connected representations of cortical gray matter for functional mri visualization," *IEEE Transactions on Medical Imaging*, vol. 16, pp. 852–863, 1997.

[6] W. S. Massey, *A Basic Course in Algebraic Topology*, Graduate Texts in Mathematics. Springer-Verlag, 1991.

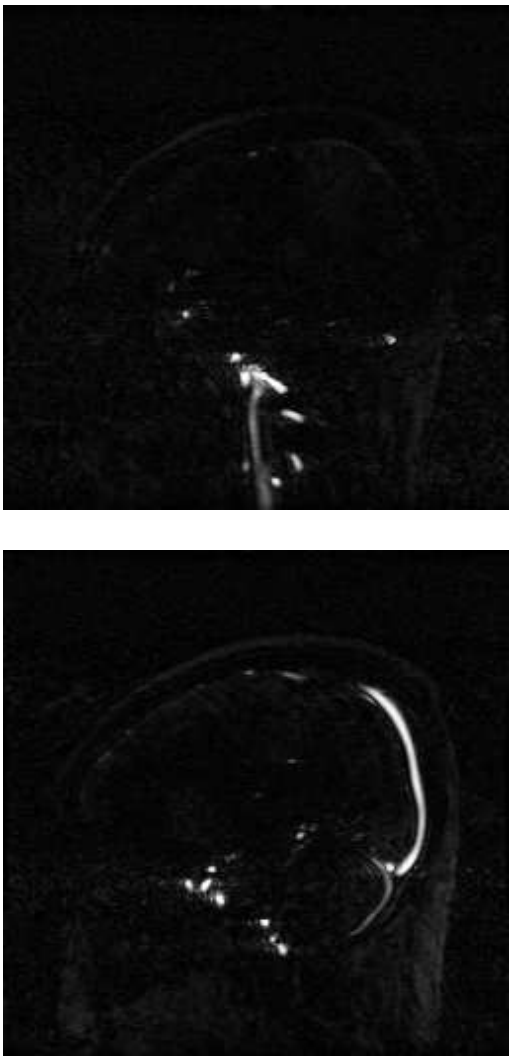

**Fig. 1**. Slices through unprocessed MRA data (the gray-value histogram was adjusted for better visibility).


[7] T. Kaczynski, K. Mischaikow, and M. Mrozek, *Computational Homology*, 2002.

[8] W. D. Kalies, K. Mischaikow, and G. Watson, "Cubical approximation and computation of homology," in *Conley Index Theory*, pp. 115–131. Banach Center Publications, 1999.

[9] M. Hirsch, *Differential Topology*, Graduate Texts in Mathematics. Springer-Verlag, 1976.

[10] T. Kaczynski, K. Mischaikow, and M. Mrozek, "Computing homology," Tech. Rep., Georgia Institute of Technology, 2001.


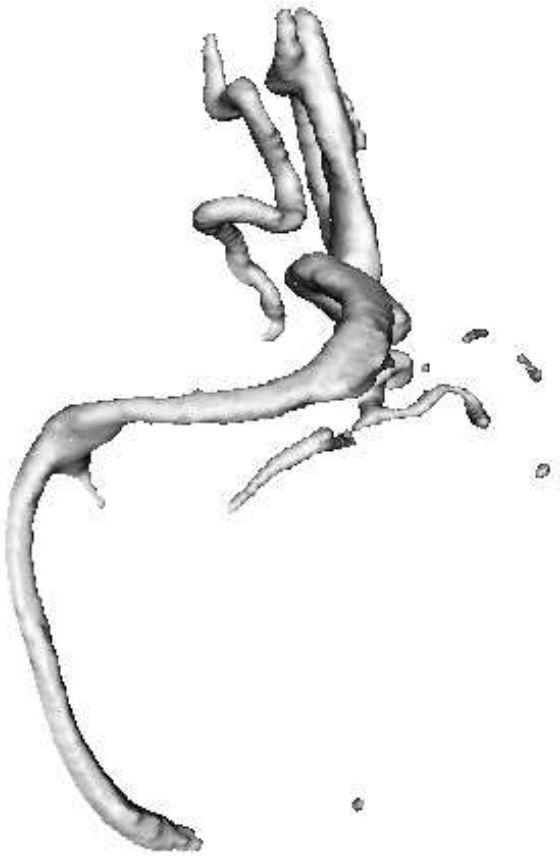

**Fig. 2**. Rendering of the segmented blood vessels.

**Fig. 3**. Skeleton of the cubical complex of the blood vessels, and one-generators.